Impact of two-photon absorption on self-phase modulation in silicon waveguides

Lianghong Yin and Govind P. Agrawal

Institute of Optics, University of Rochester, Rochester, New York 14627, USA

Received March 22, 2007; revised April 30, 2007; accepted May 1, 2007;
posted May 2, 2007 (Doc. ID 81345); published July 5, 2007

We study the effects of two-photon absorption on the self-phase modulation (SPM) process in silicon waveguides while including both free-carrier absorption and free-carrier dispersion. An analytical solution is provided in the case in which the density of generated carriers is relatively low; it is useful for estimating spectral bandwidth of pulses at low repetition rates. The free-carrier effects are studied numerically with emphasis on their role on the nonlinear phase shift and spectral broadening. We also consider how the repetition rate of a pulse train affects the SPM process. © 2007 Optical Society of America

OCIS codes: 190.4360, 130.4310.

Silicon photonics is a rapidly growing field that has made significant advances in recent years [1,2]. The nonlinear effects are enhanced considerably in silicon-on-insulator (SOI) waveguides because of the large values of the Kerr parameter and the Raman gain coefficient and the tight confinement of the optical mode. Nonlinear effects in SOI waveguides have already been exploited for Raman amplification, four-wave mixing, and soliton formation [3–6]. The phenomenon of self-phase modulation (SPM) plays an important role in most cases, as it leads to chirping and spectral broadening of ultrashort pulses [7–9]. In practice, two-photon absorption (TPA) limits the extent of SPM through nonlinear absorption and generation of free carriers that not only absorb light (free-carrier absorption, or FCA) but also modify the refractive index (free-carrier dispersion, or FCD). In this paper, we study the impact of these effects on SPM both analytically and numerically with an emphasis on the physics behind them. We also consider pulse trains to explore how the repetition rate of a pulse train affects the SPM process.

The propagation of an optical pulse through an SOI waveguide is governed by [7–10]

$$\frac{\partial E}{\partial z}+\frac{i\beta_2}{2}\frac{\partial^2 E}{\partial t^2}=ik_0n_2(1+ir)|E|^2E-\frac{\sigma}{2}(1+i\mu)N_cE-\frac{\alpha_l}{2}E, \tag{1}$$

where E is the electric-field envelope, $k_0=2\pi/\lambda$, β_2 is the dispersion parameter at the input wavelength λ, n_2 is the Kerr coefficient, σ is the FCA coefficient, and α_l accounts for linear losses. The dimensionless parameter r governs the relative importance of TPA and is defined as $r=\beta_{\mathrm{TPA}}/(2k_0n_2)$, where β_{TPA} is the TPA coefficient. The second dimensionless parameter μ governs the impact of FCD and is analogous to the linewidth enhancement factor well known in the context of semiconductor lasers. The TPA-induced free-carrier density N_c is governed by the rate equation

$$\frac{\partial N_c(z,t)}{\partial t}=\frac{\beta_{\mathrm{TPA}}}{2h\nu_0}|E(z,t)|^4-\frac{N_c(z,t)}{\tau_c}, \tag{2}$$

where $\tau_c\sim 1$ ns is the carrier lifetime [8].

The parameters appearing in Eqs. (1) and (2) depend on the carrier wavelength of the input pulses, chosen to be 1.55 μm as this spectral region is most relevant for silicon photonics. At this wavelength, $n_2\approx 6\times10^{-18}\,\mathrm{m^2/W}$, $\beta_{\mathrm{TPA}}\approx 5\times10^{-12}\,\mathrm{m/W}$, and $\sigma=1.45\times10^{-21}\,\mathrm{m^2}$ [11], resulting in $r=0.1$. The parameter μ is estimated using $\mu=2k_ck_0/\sigma$ with $k_c=1.35\times10^{-27}\,\mathrm{m^3}$ [12] and is found to be close to 7.5. A relatively large value of μ indicates that the FCD effects are important for silicon waveguides and must be included. Note that the effective values of these parameters may change for small-size waveguides [4,9].

In general, Eqs. (1) and (2) need to be solved numerically. However, under certain conditions, an approximate analytic solution is possible. First, dispersive effects can be neglected for picosecond pulses because the waveguide length is typically much shorter than the dispersion length, $L_D=T_0^2/|\beta_2|$, where T_0 is the pulse width. Second, if we assume that the repetition rate R_p of the pulses is low ($R_p\tau_c\ll 1$) and their peak intensity is not too high, N_c remains low enough that we can neglect both FCA and FCD. We estimate that N_c is negligible when the input peak intensity I_0 satisfies the condition $I_0\ll 3h\nu_0/(\sigma T_0)$. For example, $I_0\ll 2.7\,\mathrm{GW/cm^2}$ for $T_0=10$ ps. If we set $N_c=0$ and $\beta_2=0$ in Eq. (1), we get

$$\partial E/\partial z=ik_0n_2(1+ir)|E|^2E-\alpha_lE/2. \tag{3}$$

Substituting $E=\sqrt{I}\exp(i\phi-\alpha_lz/2)$ and solving the resulting equations for intensity I and phase ϕ, we get

$$I(L,t)=\frac{I(0,t)\exp(-\alpha_lL)}{1+2k_0n_2rI(0,t)L_{\mathrm{eff}}}, \tag{4a}$$

$$\phi(L,t)=(2r)^{-1}\ln[1+2k_0n_2rI(0,t)L_{\mathrm{eff}}], \tag{4b}$$

where $L_{\mathrm{eff}}=(1-e^{-\alpha_lL})/\alpha_l$ is the effective length for a waveguide of length L.

0146-9592/07/142031-3/$15.00

The preceding solution shows how the intensity and SPM are affected by the TPA parameter r. In the limit $r \to 0$ (no TPA), we recover the standard result used for fibers [13], and the maximum nonlinear phase shift at the pulse center is $\phi_{\max} = k_0 n_2 I_0 L_{\text{eff}}$. In the presence of TPA, the phase shift at the pulse center becomes $\phi_0 \equiv \phi(L,0) = \ln(1+2r\phi_{\max})/(2r)$. This phase shift is plotted in Fig. 1 as a function of $2r$ for three values of $\phi_{\max}$. As one may expect, TPA reduces the SPM-induced phase shift, and the reduction becomes more severe at higher input intensity levels because of a logarithmic growth of ϕ_0 with intensity. This logarithmic growth is seen more clearly in the inset, where we plot ϕ_0 as a function of $\phi_{\max}$ using $r = 0.1$ (the value estimated for Si at 1.55 μm) and compare it with the linear growth (dashed line). Clearly, the nonlinear phase shift is severely limited by TPA at high intensity levels.

Next we focus on the case that the input intensity level high enough that TPA-generated carriers and the associated FCA and FCD cannot be neglected. In this case, we solve Eqs. (1) and (2) numerically and focus on a specific SOI waveguide of 2 cm length with $\alpha_l = 1$ dB/cm, $\beta_2 = \pm 1$ ps^2/m, and a carrier lifetime of $\tau_c = 1$ ns [8]. The 1.55 μm input pulses have a Gaussian shape with the intensity profile $I(0,t) = I_0 \exp(-t^2/T_0^2)$. We choose $T_0 = 10$ ps. For simplicity, we first consider the case of a low repetition rate ($R_p \tau_c \ll 1$) so that free carriers generated during a pulse have sufficient time to recombine before the next pulse arrives. As a result, we can focus on a single pulse.

The top row of Fig. 2 shows the output pulse spectra at two different input intensities when all effects are included (solid curves). The first plot corresponds to $\phi_{\max} = 1.5\pi$, but $\phi_{\max} = 7.5\pi$ for the second one. The dashed curves based on the analytic solution include TPA ($r = 0.1$) but neglect free-carrier effects. Based on the limiting value of input intensity for which our analytic model holds, FCA and FCD effects are relatively small in the first case but become quite large in the second case. The dotted curves show the $r = 0$ case (no TPA). Clearly, TPA effect becomes strong enough for $I_0 = 6$ GW/cm^2 that the spectral width is reduced

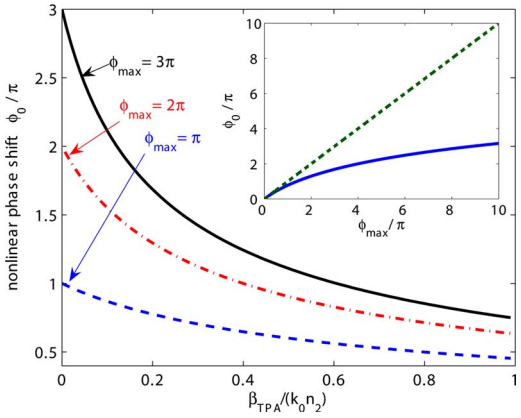

Fig. 1. (Color online) Reduction in nonlinear phase shift at the pulse center because of TPA inside a silicon waveguide for $\phi_{\max} = \pi, 2\pi$, and 3π. Inset, ϕ_0 as a function of $\phi_{\max}$ using $r = 0.1$; dashed curve, $r = 0$ case.

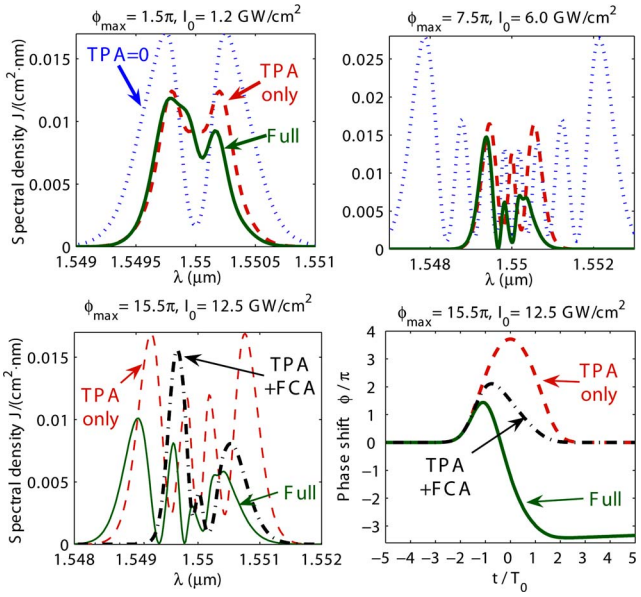

Fig. 2. (Color online) SPM-broadened pulse spectra (solid curves) at the end of a 2-cm-long SOI waveguide at three input intensities such that $\phi_{\max} = 1.5\pi$, 7.5π, and 15.5π. Dashed curves include TPA but neglect FCA and FCD effects; dotted curves neglect TPA as well. The nonlinear phase profiles in the three situations are shown in the last plot for $\phi_{\max} = 15.5\pi$.

from 5 to <2 nm. Note that our analytical model provides a reasonable estimate of the spectral bandwidth even when input intensity levels are so high that N_c is not negligible. This is so because free carriers affect mostly the spectral shape. We can use this feature to predict the spectral bandwidth analytically from Eq. (4b) [13]. The spectra in Fig. 2 also agree qualitatively with recent experiments [9].

An important feature to note in Fig. 2 is that, while TPA leaves the pulse spectrum symmetric, the free carriers produced by TPA make it considerably asymmetric. In particular, free carriers affect mostly the "red" part of the spectrum; the "blue" part remains almost unchanged at low intensity levels. The question is whether this asymmetry is introduced by FCA, FCD, or both of them. To answer this question, we show in Fig. 2(c) pulse spectra at an intensity level of 12.5 GW/cm^2 under the influence of TPA only (dashed curve), TPA and FCA (dotted–dashed curve), and all three effects (solid curve). The spectrum becomes narrower and asymmetric when FCA is included without FCD ($\mu = 0$). The effect of FCD ($\mu = 7.5$) is to broaden the spectrum and shift it toward the "blue" side. To understand these features, we show in Fig. 2(d), the nonlinear phase shift across the pulse in the three cases. The phase profile is symmetric in the case of TPA only, becomes asymmetric when FCA is included, and develops negative values in the pulse tails when FCD is included.

Physically, changes in the nonlinear phase shift result from the time-dependent nature of the carrier-density buildup at any point in the waveguide. Near the leading edge of the pulse, $N_c \approx 0$. As the pulse passes through that location, N_c builds up and continues to increase even after the pulse peak has

passed. We can estimate the profile of $N_c(t)$ by solving Eq. (2) approximately near the front end of the waveguide where $|E(z,t)|^2$ is close to its input. Noting that pulse width $T_0 \ll \tau_c$, the τ_c term can be ignored as carriers do not have enough time to recombine over the pulse duration. The carrier density is then given by

$$N_c(t) \approx \frac{\beta_{\mathrm{TPA}} I_0^2 T_0}{2h\nu_0} \sqrt{\frac{\pi}{8}} \left[1 + \mathrm{erf}\left(\frac{\sqrt{2}t}{T_0} \right) \right]. \qquad (5)$$

After the pulse has passed through the input end, $N_c \approx 3 \times 10^{18}\ \mathrm{cm}^{-3}$ for the parameter values used in our study. Absorption by these carriers reduces the phase shift in an asymmetric fashion, as seen by the dotted–dashed curve in Fig. 2(d).

To understand the role of FCD, we first note that the FCD-induced phase shift has a sign opposite to that of the Kerr effect as seen in Eq. (1). This can be understood by noting that free carriers reduce the refractive index while the Kerr effect increases it. Physically speaking, the total nonlinear phase shift ϕ has contributions from these two effects [10]. Because of the opposite signs associated with them, the total nonlinear phase shift is reduced all across the pulse (compared with the TPA only situation). In particular, ϕ becomes 0 at a certain time and negative after that, as shown clearly in Fig. 2(d). The blueshift seen in Fig. 2(c) originates from such negative values of ϕ. The pulse spectrum broadens because of FCD (compared with the dotted–dashed curve) because ϕ changes rapidly over a short time interval.

We next consider the impact of repetition rate R_p associated with a pulse train on SPM-induced spectral broadening. The important dimensionless parameter is $R_p\tau_c$. As long as $R_p\tau_c \ll 1$, the preceding results shown in Fig. 2 remains reasonably accurate. However, if $R_p\tau_c$ is close to or exceeds 1, the situation changes dramatically because carriers produced by a pulse do not have enough time to recombine before the next pulse arrives. As a result, the density of carriers from pulse to pulse increases until a steady state is reached. In numerical simulations, we obtain this steady-state value by propagating a large number of pulses. The characteristic time needed to reach the steady state is 4–5 τ_c. Since $N_c(z,t)$ then follows a periodic pattern, we can focus on one pulse.

Figure 3 shows the pulse spectra at three intensity levels under conditions identical to those in Fig. 2 except that all effects are included and the pulse repetition rate is changed from a relatively low value of 10 MHz to a relatively high value of 10 GHz. The 10 MHz curves (solid) are identical to those shown in Fig. 2 as $R_p\tau_c = 0.01$ for them. The 1 GHz curves (dashed) represent the intermediate case of $R_p\tau_c = 1$. The 10 GHz case (dotted–dashed) corresponds to $R_p\tau_c = 10$ and represents the worst-case scenario in which the background value of the carrier density becomes excessively large. The main conclusion is that the parameter $R_p\tau_c$ should be ≤ 0.2 if SPM-induced spectral broadening is desirable. In practical terms, the carrier lifetime should be reduced to below 20 ps if the SOI waveguide is to operate at a bit rate of 10 Gbits/s, which is used commonly for telecommunication applications. One way to reduce the carrier lifetime is to use a reverse-biased p-i-n diode structure to remove the carriers [5].

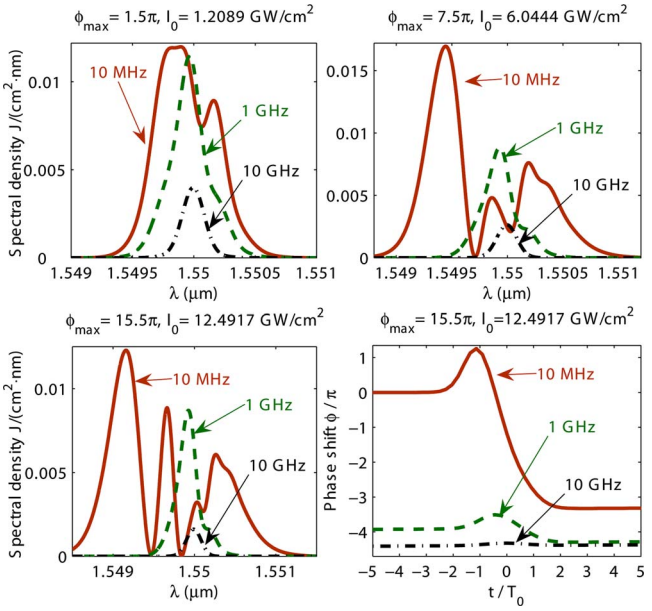

Fig. 3. (Color online) Pulse spectra at the same three intensity levels as in Fig. 2 except that all effects are included and three repetition rates are considered. The nonlinear phase shift at three different repetition rates is shown in part (d) at $I_0 = 12.5\ \mathrm{GW/cm^2}$.

In summary, we have presented a comprehensive study of the SPM phenomenon in SOI waveguides in the presence of the TPA, FCA, and FCD effects. The FCA and FCD effects are studied numerically for a better understanding of their role on SPM-induced chirping and spectral broadening. We also studied how the repetition rate of a pulse train affects the SPM process.

References

1. M. Lipson, J. Lightwave Technol. **23**, 4222 (2005).
2. L. Pavesi and D. J. Lockwood, *Silicon Photonics* (Springer, 2004).
3. R. Claps, D. Dimitropoulos, V. Raghumathan, Y. Han, and B. Jalali, Opt. Express **11**, 1731 (2003).
4. X. Chen, N. C. Panoiu, and R. M. Osgood, IEEE J. Quantum Electron. **42**, 160 (2006).
5. H. Rong, Y. Kuo, A. Liu, M. Paniccia, and O. Cohen, Opt. Express **14**, 1182 (2006).
6. L. Yin, Q. Lin, and G. P. Agrawal, Opt. Lett. **31**, 1295 (2006).
7. G. W. Rieger, K. S. Virk, and J. F. Young, Appl. Phys. Lett. **84**, 900 (2004).
8. O. Boyraz, P. Koonath, V. Raghunathan, and B. Jalali, Opt. Express **12**, 4094 (2004).
9. I. Hsieh, X. Chen, J. I. Dadap, N. C. Panoiu, and R. M. Osgood, Opt. Express **14**, 12380 (2006).
10. R. Dekker, A. Driessen, T. Wahlbrink, J. Niehusmann, and M. Först, Opt. Express **14**, 8336 (2006).
11. H. K. Tsang, C. S. Wong, T. K. Liang, I. E. Day, S. W. Roberts, A. Harpin, J. Drake, and M. Asghari, Appl. Phys. Lett. **80**, 416 (2002).
12. Q. Xu and M. Lipson, Opt. Lett. **81**, 341 (2006).
13. G. P. Agrawal, *Nonlinear Fiber Optics*, 4th ed. (Academic, 2007).